La mer 30: 275–285, 1992
Société franco-japonaise d'océanographie, Tokyo

Wave characteristics changes under a strong tidal current influence

Im Sang OH and Yoo Yin KIM*

Abstract: It is well known that a strong current influences a wave field in several ways, such as frequency shift, amplitude changes. In the present study, we reexamined the influences of current on a wave field in a theoretical point of view in the first half of this paper. In the next half, we compared the observed wave heights with the computed wave heights with tidal currents. We also compared the computed wave spectra with tidal currents and those wihout tidal currents. The wave measurements are conducted at the Maldo Island from Nov. 7 to Nov. 10, 1990, which is located in the west coastal area of Korea. For the computations, Shallow Water Wave model (SWW model : OH *et al.*, 1990) was used.

In the typical range of tidal currents and elevation of the Maldo area, the influence of tidal currents on waves is large than that of tidal elevations, i.e., water depth changes of the ranges. For the area, the observed wave heights show considerable differences from those with current. The difference may be larger in some areas with stronger tidal currents. The model calculations show 7–12% difference in the wave energy spectra with and without currents in the shallow water wave model.

1. Introduction

A wave field in some area can be strongly influenced by steady or variable currents if the currents of the area are strong. In those areas, the current should be considered in estimating the wave energy. The Yellow Sea is an area of this kind.

There are several ways that a horizontal current can modify surface gravity waves. One way of modifications is to wavelength. A current can locally stretch or shrink features in a wave train. This wave train distortion produces a "Doppler shift" in wave period. Another way is to wave orthogonals. Wave orthogonal is a line perpendicular to the local wave crest direction. In this study the wave refraction due to tidal currents is not considered since the wave refraction due to tidal currents is generally much smaller than that due to water depth variations.

Another type of modification occurs also in the pressure field accompanying waves. This change can be an appreciable source of error in measuring wave heights or periods if an existing current is not accounted for. In particular, a significant error can sometimes arise if bottom pressure measurements are used to determine surface wave heights and lengths.

The studies of wave-current interaction, in particular the influence of currents on waves, have been done extensively in the past decades (Interested readers refer to PHILLIPS (1969), PEREGRINE (1976) and THOMAS (1981) for their detailed and comprehensive reviews of waves on currents). The followings are the brief reviews of the studies.

A significant theoretical advance of wave-current interaction was achieved by LONGUET-HIGGINS and STEWART (1960, 1961), who introduced the concept of radiation stress. A year later, WHITHAM (1962) introduced so-called Whitham's method which uses the averaged Lagrangian and the concept of wave action. PHILLIPS (1969) formulated a wave spectral transformation on currents theoretically in water of finite depth, and showed that the spectral energy density in the wavenumber space is constant following a wave group.

HUANG *et al.* (1972) showed the relative changes of spectral energy ($\bar{\phi}$) under different

* Department of Oceanography, Seoul National University, Seoul 151–742, Korea

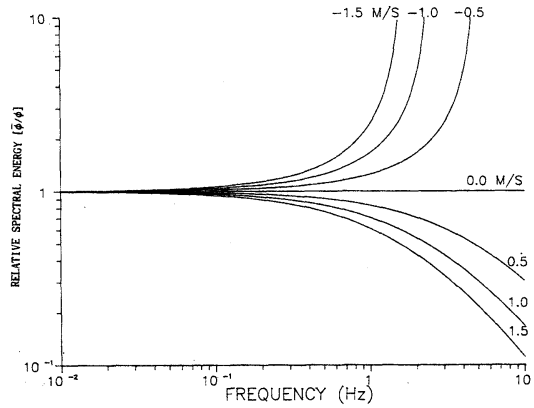

Fig. 1. Relative changes of frequency spectra under different current conditions (HUANG *et al.*, 1972).

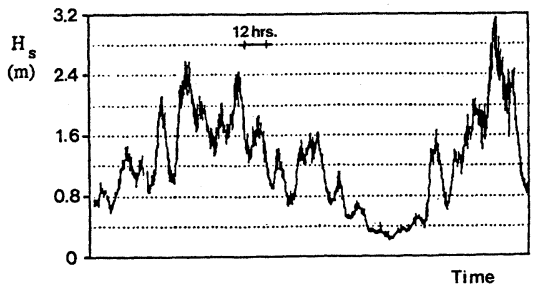

Fig. 2. Measured significant wave height H_s (TOLMAN, 1990).

current conditions to the Kitaigorodskii-Pierson-Moskowitz frequency spectrum (ϕ) as the basic spectral form for zero current condition (Fig. 1).

The interaction between wind-generated surface waves and tidal currents (VINCENT, 1979), the effect of tidal currents on the velocity spectrum (LAMBRAKOS, 1981), and the influences of unsteady currents on wind wave propagation on the scale of shelf scale (TOLMAN, 1990) are also studied. TOLMAN showed that a wave height modulation is up to 50 % with a period of approximately 12 hours in the Southern North Sea (Fig. 2). Numerical method (WANG and YANG, 1981) and laboratory experiments (LAI *et al.*, 1989) are also applied to the study of current effects.

In the present study, we reexamined the influence of strong currents on a wave field. At the same time, we measured the wave heights and tidal currents at the Maldo from Nov. 7 to Nov. 10, 1990 (See Fig. 3 for the location and bottom contours of the Maldo area). The wave fields for the period are simulated by using Shallow Water Wave model (SWW model: OH *et al.*, 1990). The computed wave heights with considering tidal currents are compared with the observed ones. The computed wave spectra with and without tidal currents are also compared in order to estimate the order of magnitudes of the influence of currents on wave field.

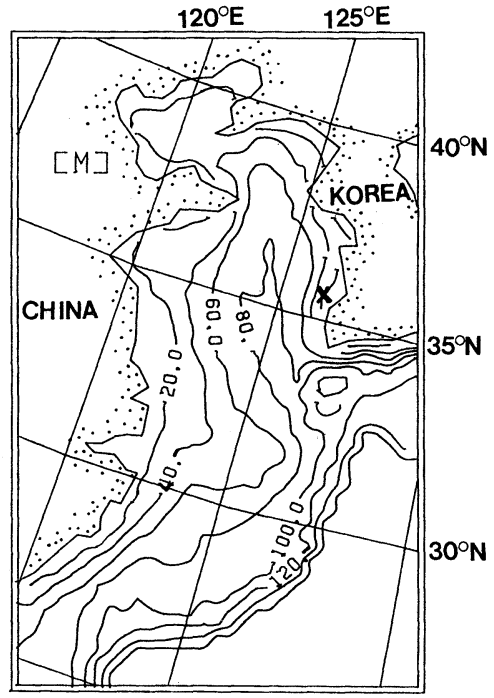

Fig. 3. Location of the experimental site (point x), Maldo area and the depth contours of the Yellow Sea.

2. Theoretical considerations

a. Steadiness of Tidal Current

It is necessary to have a clear appreciation of the relative magnitude of time and length scales for both the waves and the currents for a better understanding of their interactions. A large-scale current, such as a tidal current, might be an example which varies very little, say, no more than a few percent over a distance of one wavelength, L, or over a time of one wave period, T.

Waves, however, propagate over a tidal current for a considerably long time. Then the

variability of the current must be accounted. The critical period of a current, the semidirunal tide, for example, can be estimated as

$$T_c = |U_{\max}| / |\partial U / \partial t|_{\max} \quad (1)$$

when the tidal current $U(t) = U_{\max} \sin(\omega t)$ is assumed. Here, $U_{\max}$ and ω are the maximum speed and the tidal frequency, respectively. Considering the tidal component M_2 for the Maldo area, we get $T_c \simeq 2$ hour. Thus, if waves are propagating over the tidal currents for more than two hours, the unsteadiness of the current needs to be considered, and if a propagation time is less than T_c the tidal current can be considered as a steady current.

b. Effect of the Presence of Current on Wave Field

If a wave train is propagating in a medium moving with velocity $U(u, v; \vec{x}, t)$, the frequency of waves passing a fixed point, apparent frequency ω, is given by

$$\omega = \vec{k}\, U(\vec{x}, t) + \sigma(\vec{k}, h) \quad (2)$$

where σ is the intrinsic frequency whose functional dependence on wave number $\vec{k}$ and water depth h is known as the dispersion relation. If the nonlinear dynamic interaction is neglected, the dispersion relation is of the form:

$$\sigma^2 = gk \tanh(kh) \quad (3)$$

where g is the gravity, $k = |\vec{k}|$. From (3) we have the relative wave phase speed C_0 as

$$C_0 = [(g/k) \tanh(kh)]^{1/2} \quad (4)$$

and the absolute phase speed C_a is given by

$$C_a = C_0 + U \quad (5)$$

If the water depth h, intrinsic frequency σ, and the current speed and direction of U are known, we can calculate the wave number of no current by (3) and apparent frequency ω by (2), and then the wave number under current influence can be determined as follows.

$$\omega = [gk \tanh(kh)]^{1/2} + uk \cos\theta + vk \sin\theta \quad (6)$$

where u, v are component currents in x- and y-direction, respectively, and θ is the angle between the wave-ray and x-axis.

c. Combined Effects of Current and Water Depth on Wave Field

The changes of wave lengths, phase speeds and Doppler frequencies for variable water depths are shown in Fig. 4 for each effective tidal current speed giving influence to the wind waves. The positive tidal current speed means that the current flows in the same direction as the waves do, i.e., co-current. For this computation, we used the combined form of dispersion relations of (2) and (3). The figure shows that the wave length, phase velocity, and Doppler frequency with co-currents are larger than those with counter-currents. In general, the influence of counter-currents on waves is larger than that of co-currents as we expected.

It is worthwhile to note that if we consider the typical ranges of tidal currents and elevations for the study area are 1.5 m/s and 5 m, respectively, the influence of tidal currents on waves is larger than that of tidal elevations, i.e., water depth changes of the ranges.

Fig. 5 shows the relations between the apparent frequency ω and wave number k. When there is no current, k_{o1}, k_{o2}, and k_{o3} are the wave numbers for constant water depths, h_1, h_2, and h_3, respectively. ω_0 is the frequency of no current. If there exists a flow U which is against the wave propagation direction, U can be considered as a slope for the linear equation for k. Thus, the left hand side of the equation will be a line whose slope is U and its cross section is ω_0 in ω-k plane. The values k_1, k_2, and k_3 at which the line crosses the curves of constant depths h_1, h_2, and h_3, respectively, are the wave numbers, and ω is the frequency in common for the wave numbers.

If there exists an opposing current, two solutions for k can be found. These solutions converse to k_c as U increases. The wave number k_c is called as a critical wave number. The frequency ω_c is a critical frequency at the critical wave number k_c.

In the range of wave number bigger than the

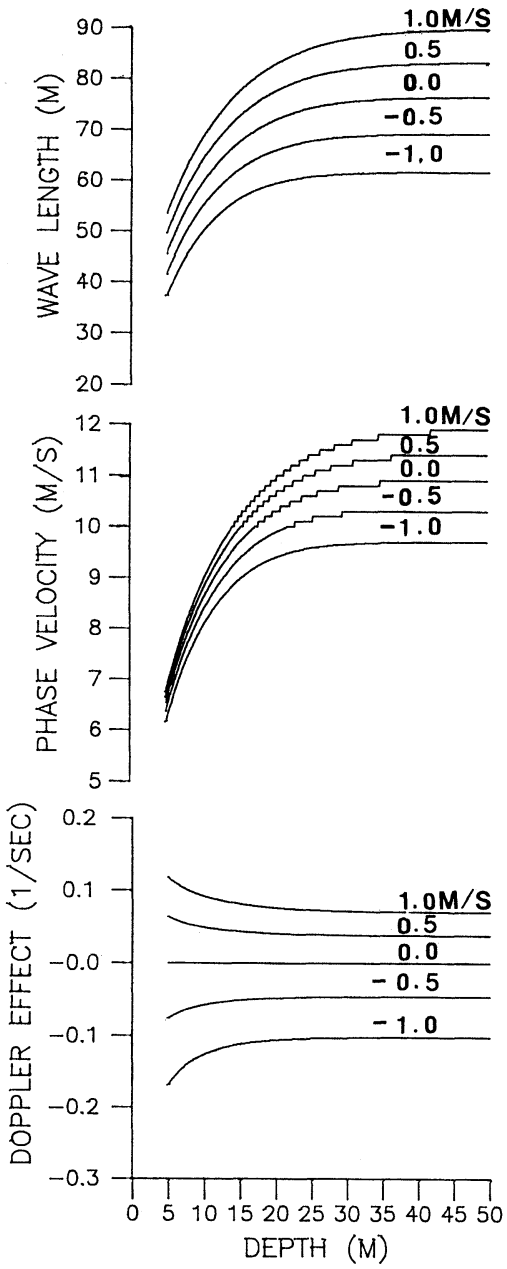

Fig. 4. Variations of wave length, phase velocity and Doppler effect depending upon water depth and effective current speed changes.

critical wave number k_c, when the flow U increases, the solutions for k and the corresponding frequency decrease to k_c and ω_c, thus, the wave lengths and period increase. In the wave number range smaller than k_c, the solution and corresponding frequency increases to converge

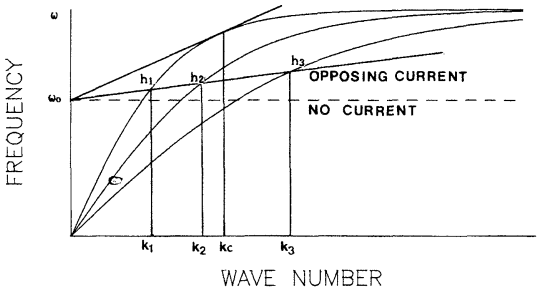

Fig. 5. Wave number and frequency relationship with opposing current.

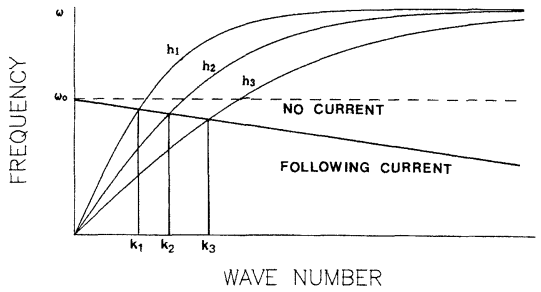

Fig. 6. Wave number and frequency relationship with following current.

to k_c and ω_c. The wave lengths and the period decrease. In this range, the changing rate of wave number increases as the current increases and as the water depth decreases.

Fig. 6 shows the ω-k solution for the case of co-current, in which the direction of wave propagation is identical to the current. In this case, since the solution for k and the corresponding frequency are always smaller than those of no-current, the wave lengths and period become longer. The changing rate of the wave numbers increases as the water depth decreases.

3. Comparisons of spectra with and without currents

In order to investigate the influences on wind waves due to tide, we measured wave heights and tidal currents at the Maldo area (See Fig.3) for the period of Nov. 7 to Nov. 10, 1991. The instrument used for the measurements is a multi-functional pressure type gauge which can measure wave heights, tides and their current directions and speeds. It was moored at the sea bottom of 20 m depth.

Wind speeds and tidal currents during the measurement period for the whole Yellow Sea

are simulated. Using these wind and tidal current data wave heights are calculated by the Shallow Water Wave model (SWW model: OH *et al.*, 1990). In the following two subsections, the models are briefly explained.

a. Shallow Water Wave model

In shallow water, the wave train will have new experiences such as strong tidal currents with rapid variations of water depth, bottom friction, refraction, shoaling, and wave breaking. The present SWW model includes those effects in calculations. We chose this model because it has been applied to the present study area successfully (OH *et al*, 1990). The model uses a prefixed grid system and a finite difference method with a jumped technique. It has 208 component waves : 13 classes of wave period and 16 classes of propagation direction. It utilizes HASSELMANN (1960)'s idea. According to him, the development of an angular spectral density $E\ (T, \theta, x, y, t)$ can be described by the following relation,

$$\frac{dE(T, \theta, x, y, t)}{dt} = S(T, \theta, x, y, t) \qquad (7)$$

where S is a source function for the wave field, and T, t and θ are wave period, time and wave propagation direction, respectively. Since the group velocity and the propagation direction change as the energy of each component wave moves, the energy equation should be expressed as,

$$\frac{dE}{dt} = \frac{\partial E}{\partial t} + \frac{\partial E}{\partial x}\frac{dx}{dt} + \frac{\partial E}{\partial y}\frac{dy}{dt} + \frac{\partial E}{\partial T}\frac{dT}{dt} + \frac{\partial E}{\partial \theta}\frac{d\theta}{dt} = S \qquad (8)$$

We converted this into an equation which can be used for the computations of wave energy along a wave ray. If we assume the wave period is conserved, the energy balance equation becomes

$$\frac{dE}{dt} = \frac{\partial E}{\partial t} + \frac{\partial E}{\partial s}\frac{dS}{dt} + \frac{\partial E}{\partial \theta}\frac{d\theta}{dt} = S_{in} + S_{ds} + S_{bf} \qquad (9)$$

where the source function of the right hand side consists of S_{in}, energy input from wind field, S_{ds}, energy loss due to viscosity and breaking, and S_{bf}, energy dissipation due to bottom friction. For the energy input, the formula which is used by GELCI and DEVILLAZ (1975) in their DSA-5 wave model, is utilized in the present study. The energy loss due to viscosity is considered by assuming the eddy viscosity coefficient is proportional to the total wave energy. The total time derivative of the wave energy of a component wave, $E_{T,\theta}$, is

$$\frac{dE_{T,\theta}}{dt} = I - AE_{T,\theta} \qquad (10)$$

where the energy input due to wind, I is

$$I = \int_{\text{component}} \int \frac{C_{in}T^2(W-2T)^3}{W^3}\frac{2}{\pi}\cos^2(\theta-\phi)\, dT\, d(\theta-\phi), \qquad (11)$$

and

$$A = 18\times10^{-9}E_{tot} \qquad (12)$$

Here, W is the wind speed in knot, ϕ the wind direction, and E_{tot} is the sum of all the componental waves.

Energy dissipation due to bottom friction is also considered by utilizing COLLINS (1972) model. The bottom frictional energy dissipation is assumed to be proportional to the mean water particle velocity and to the frequency-directional spectrum. S_{bf} is

$$S_{bf} = C_f \alpha(T,h)\ \langle V\rangle\ E(T,\theta) \qquad (13)$$

where C_f is the bottom friction coefficient, $\alpha\ (T,h) = gkC_g/(2\pi\sigma^2\cosh^2 kh)$, C_g the group velocity, and $\langle V\rangle$ is the ensemble average of a water particle velocity of water depth h.

Wave breaking due to water depth is included by using a simple formula by YOUNG (1988) as

$$E_{\max} = 0.0355\ h^2 \qquad (14)$$

The $E_{\max}$ is the maximum possible total energy at a computational grid point. If the total energy is greater than $E_{\max}$, then the excess energy is drained from the longer wavelength component first.

The computation is conducted in the following

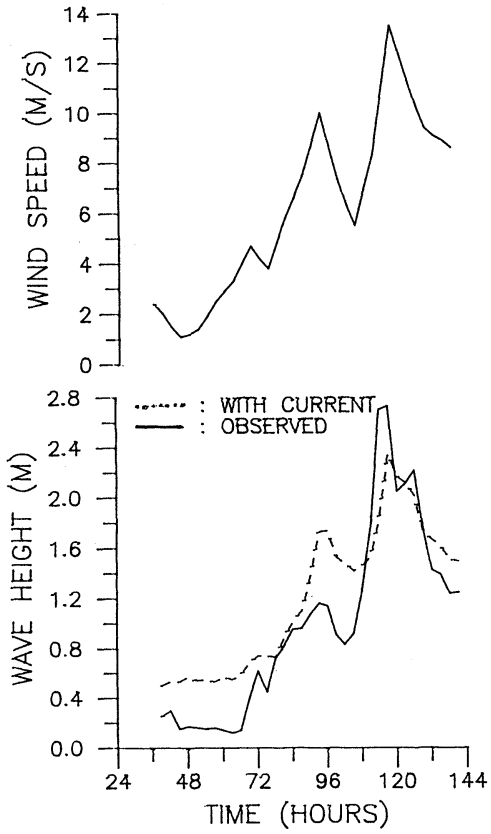

Fig. 7. Computed wind speed (upper), and the observed and the computed wave heights (lower) for the Maldo from Nov. 7 to Nov. 10, 1990.

order by using the former step's result as an input

$$\left[\left[\left[\frac{dE}{dt}=S_{in}+S_{ds}\right]_{i}+S_{bf}\right]_{ii}-\frac{\partial E}{\partial s}\frac{ds}{dt}\right]_{iii} - \frac{\partial E}{\partial \theta}\frac{d\theta}{dt}\Big]_{iv} \quad (15)$$

More detailed descriptions may be found in OH *et al.*(1990).

Precalculated tidal currents were used in the model by equation (6). New frequency was calculated for all the wave components at each grid point (i, j).

$$\omega_{ij}=[gk_{ij}\tanh(k_{ij}h_{ij})]^{1/2}+u_{ij}k_{ij}\cos\theta_{ij} + v_{ij}k_{ij}\sin\theta_{ij} \quad (16)$$

The SWW model runs on the assumption that wind velocities and tidal currents are consistent

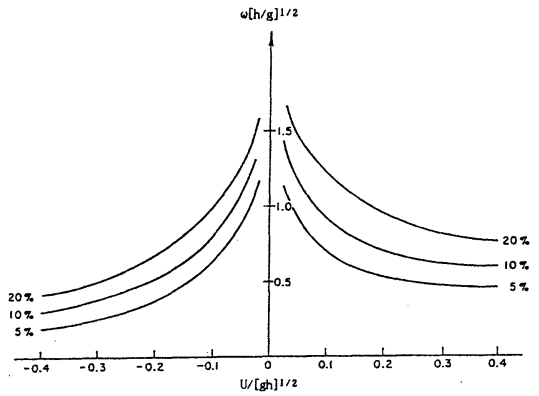

Fig. 8. Relative errors in surface wave amplitude calculated from bottom pressures due to neglect of a current component parallel with the wave direction (PERIGRINE, 1976).

for 3 hours. The tidal constituent M_2 which is dominant in the Yellow Sea is the only component considered for the tidal current computations.

b. Sea Surface Wind Model and Tidal Current Model

The sea surface wind model used in the present study is the one which was developed by BONG *et al.* (1987, 1988, 1989, 1990). The model is based on CARDONE (1969, 1978). According to him, at the upper limit of the Ekman layer the wind velocity becomes the geostrophic wind, and in surface layer the wind velocity has a logarithmic profile and it vanishes at the surface. The model is a finite difference model which utilizes iterative technique for solution. In order to run the model, the pressure distributions of 12-hour interval weather charts for the period of wave measurement at the Maldo (Nov. 7–Nov. 10, 1991) were read, and they were interpolated to make 3-hour interval data. The sea level pressure and land surface temperature were also read from the same weather charts, and monthly mean sea surface temperatures were used for this period. The irregular data such as air pressure, air temperature, etc., were rearranged to a regular grid field by using an objective analysis technique (BARNSE, 1964).

A modified tidal current model from FLATHER and HEAPS (1975) was used to obtain tidal current fields for the measurement period. The tidal model is a finite difference depth-averaged

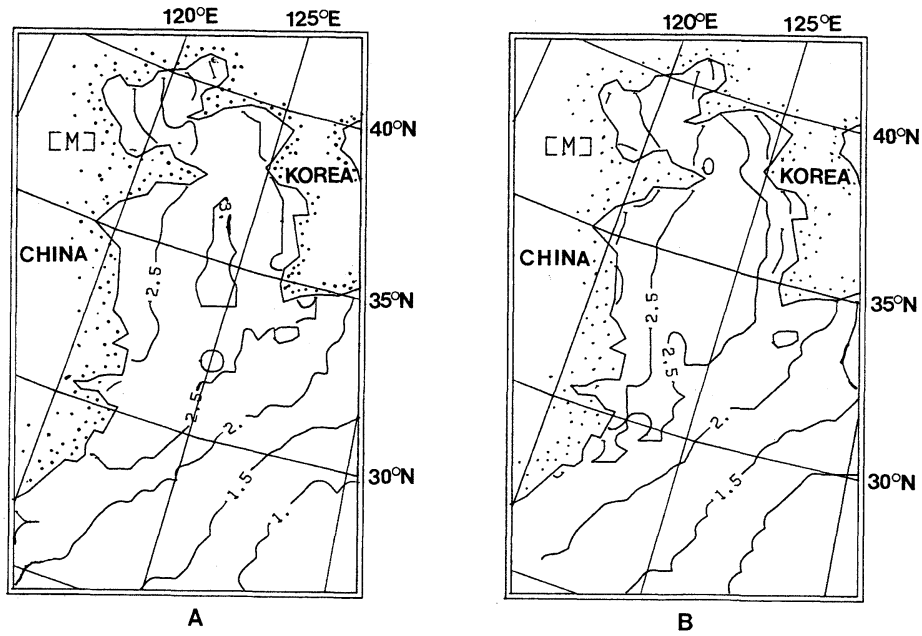

Fig. 9. Computed wave height contours with counter-directional tidal current (a) for the area near the Maldo, and without tidal current (b) at near the peak time of the measured wave energy.

model. For the open boundaries, the tidal phases and elevations of OGURA (1933, See CHOI, 1980) were used. From this model, 3-hour interval tidal currents and elevations of the M_2 component are obtained for the present wave-current interaction calculations.

c. Comparisons of waves with and without currents

The computed 3-hour interval winds and tidal currents from the SSW model and tidal current model were supplied to run the SWW model in order to see the effects of tidal currents on wind wave field. We ran the SWW model more than 144 hours.

The upper part of Fig.7 shows computed wind speeds over the Maldo area for the whole measurement period (Nov. 7 to Nov. 10, 1990). The lower part of Fig. 7 shows the observed and computed wave heights for the period. The time series of the wind speed and wave heights show a good agreement in a general tendency. Considerable discrepancy between the observed and calculated wave heights as much as 65 cm, however, appeared at the 90th hour. This discrepancy may be due to the deviation of the pressure measurements at the sea bottom in the presence of current from those of no-wind (See JONSSON *et al.*, 1970; DRAPER, 1957; PERIGRINE, 1976). Following is Perigrine's derivation. If a Fourier component of a pressure fluctuation at a bottom $z=-h$ has amplitude $p(\omega)$, then the corresponding surface amplitude component is

$$a(\omega)=p(\omega)\cosh(kh)/\rho g \tag{17}$$

The maximum errors will clearly occur when wave direction is parallel or antiparallel to a current. He also derived the following relationship: the ratio of the corrected amplitude a_2 to the computed amplitude a_1

$$\frac{a_2}{a_1}=\frac{\cosh(r)}{\cosh(q)} \tag{18}$$

where q and r are kh for the case of no-current and that for the case of current speed U, respectively. Fig. 8 shows the relative error $(a_2-a_1)/a_1$. It is easy to find from the figure that adverse currents have greater effects.

The computed wave height distribution with counter-current is shown in Fig. 9(a) and that without tidal current in Fig. 9(b) at nearly the time of energy peak when the SWW model ran for 117 hours. The area where we have interests

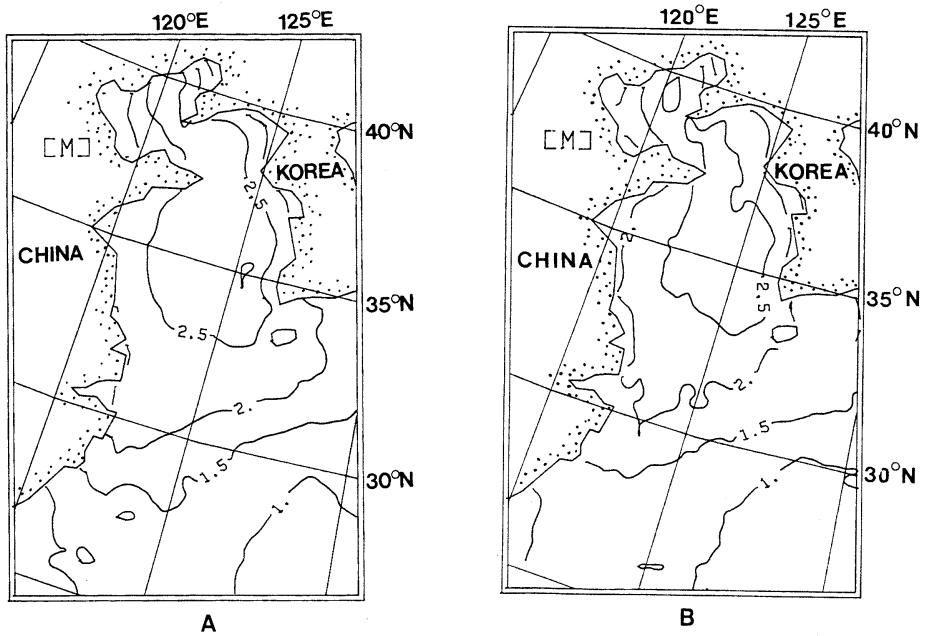

Fig. 10. Computed wave height contours with co-directional tidal current (a) for the area near the Maldo, and without tidal current (b) at nearly the peak time of the measured wave energy.

is the sea around the Maldo Island. We chose a moment when the directions of dominant tidal current and wind are the same as the direction of the significant wave propagation. The area which has wave height of 3.0 m or higher is widened when current effect is included. The general pattern, however, is similar in both cases.

The computed wave height distribution with co-current is shown in Fig. 10(a) and that without tidal current in Fig. 10(b) at nearly the time of energy peak. Similarly to Fig. 9., the area where the wave height is 2.9 m or higher is widened in the southwest of the Korean Peninsula when current effect is included. But, the area of 2.7 m or higher waveheight is shrinked. The general patterns for the both cases, however, are similar.

Fig. 11 shows the directional spectra of wave energy at the Maldo with co-currents (a) and without tidal currents (b). We notice that the dominant direction of wave is not changed but the concentration of wave energy with co-current is much more effective than that with no-current. Fig. 11(c) shows their frequency spectra. We also see the differences in spectral density of wave energy at peak frequency. Fig. 12 shows the directional spectra of wave energy at the Maldo with counter-currents (a) and without tidal currents (b), and frequency spectrum (c). Similarly to Fig. 11, the dominant direction of wave is not changed but the concentration of wave energy with counter-current is much more effective than that with no-current. We also see the considerable differences in spectral density of wave enrgy at peak frequency. Comparing the energy density spectra with co- and counter- currents, we could easily find that there exists more significant difference in the case of counter-current. From this, we can find that the wave height with tidal currents shows 7–12 % difference from the wave height without considering tidal currents.

4. Summary

The influences of steady current on a wave field are reexamined in a theoretical point of view in the first half of this paper. In the next half, we compared the observed wave heights with the computed wave heights with tidal currents. The Shallow Water Wave model is used for the computations. We also compared the wave spectra with and without tidal currents.

The results are summarized as follows.

i) Wave fields are influenced by the current

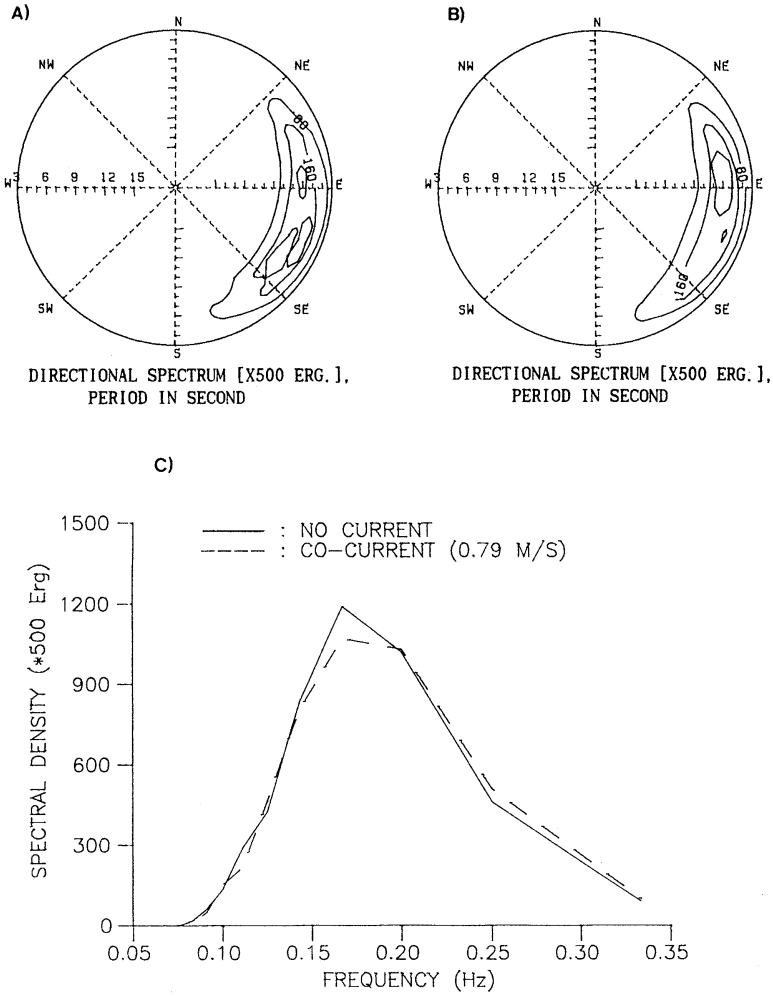

Fig. 11. Directional energy spectrum with counter-directional tidal current (a), spectum without tides (b), and frequency spectrum (c) of the Maldo area at nearly the peak time of the measured wave energy.

direction as well as magnitude. The direction and magnitude of tidal current of the Yellow Sea change in the time scale of the order of an hour; thus the wave field should be influenced by the current variations.

ii) In the typical range of tidal currents and elevation of the Maldo area, the influence of tidal currents on waves is larger than that of tidal elevations, i.e., water depth changes of the ranges.

iii) If there exists an opposing current to the wave propagation, two different wave groups can be excited. The wave numbers of the two group converges to the critical wave number as the current increases.

iv) If the current direction agrees with the wave direction, only one wave group is excited and the wave number and corresponding frequency are always smaller than those of no-current.

v) For the Maldo area, the computed spectra with tidal currents are considerably different from those without currents. The differences may be larger in some areas where tidal currents are strong.

vi) The energy density spectra with counter-currents, compared with those of no-currents, show more significant differences than the spectra with co-currents.

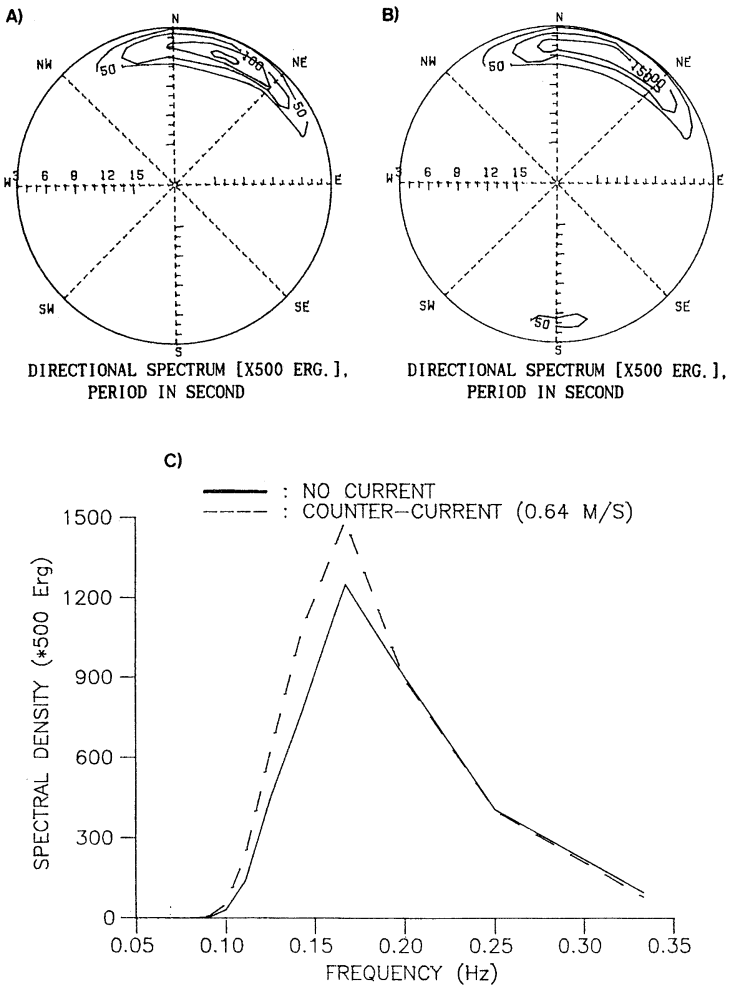

Fig. 12. Directional energy spectrum with co-directional tidal current (a), spectrum without tides (b), and frequency spectrum (c) of the Maldo area at nearly the peak time of the measured wave energy.

vii) Model calculations show 7–12% difference in the wave heights with and without currents in the model.

Acknowledgements

This study was supported by the Korea Science and Engineering Foundation through grants of 1990/1991. The authors would like to thank two anonymous reviewers who made several helpful comments and critics.

References

BARNSE, S.L. (1964): A technique for maximizing details in numerical weather map analysis. J. Meteor., **3**, 396–409.

BONG, J.H., J.B. CHOI, I.S. OH, I.S. KANG (1987): The study of meteorological characteristics and marine forecasting over the seas around Korea (I). Korea Meteorological Service, Meteorol. Res. Inst., Report 220 pp.

BONG, J.H., J.B. CHOI, I.S. OH, I.S. KANG, (1988): The study of meteorological characteristics and marine forecasting over the seas around Korea (II). Korea Meteorological Service, Meteorol. Res. Inst., Report 323 pp.

BONG, J.H., J.B. CHOI, I.S. OH, I.S. KANG, (1989): The study of meteorological characteristics and marine forecasting over the seas around Korea (III). Korea Meteorological Service,

Meteorol. Res. Inst., Report 355 pp.

BONG, J.H., J.B. CHOI, I.S. OH, I.S. KANG, (1990): The study of meteorological characteristics and marine forecasting over the seas around Korea (IV). Korea Meteorological Service, Meteorol. Res. Inst., Report 373 pp.

CARDONE, V. J. (1969): Specification of the wind distribution in the marine boundary layer for wave forecasting, New York Univ. School of Engineering and Science, Report GSL-TR 69-1, 181 pp.

CARDONE, V. J. (1978): Specification and prediction of the vector wind on the United States continental shelf for application to an oil slick trajectory forecast program. New York Univ., Institutes of Marine and Atmospheric Science, Contract T-35430.

CHOI, B. H. (1980): A tidal model of the Yellow Sea and the Eastern China Sea. KORDI Report BSPI 00019(3)-36-2.

COLLINS, J. I. (1972): Prediction of shallow water wave spectra. J. Geophys. Res., **86(C11)**, 2693-2707.

DRAPER, L. (1957): Attenuation of sea waves with depth. La Houille Blanche, **12**, 926-931.

FLATHER, R. A. and N. S. HEAPS (1975): Tidal computation for Morecamble Bay. Geophys. J. R. Astr. Soc., **42**, 489-517.

GELCI, R., and E. DEVILLAZ (1975): Le calcul numérique de l'état de la mer. La Météorologie, VI ème série, No. 2.

HASSELMANN, K. (1960): Grundleichungen der Seegangsveraussage. Schiffstechnik, 7, 191-195.

HUANG, N. E., D. T. HUANG, C.-C. TUNG, and J. R. SMITH (1972): Interactions between steady non uniform currents and gravity waves with applications for current measurements. J. Phys. Oceanogr., **2**, 420-431.

JONSSON, I. G., C. SKOUGAARD and J. D. WANG (1970): Interaction between waves and currents. Proc. 12th Coastal Engrg. Conf. **1**, 489-507.

LAI, R. J., S. R. LONG, and N. E. HUANG (1989): Laboratory studies of wave-current interaction; Kinematics of the strong interaction. J. Geophys. Res., **94**, 16201-16214.

LAMBRAKOS, K. F. (1981): Wave-current interaction effects on water velocity and surface wave spectra. J. Geophys. Res., **86**, 10955-10960.

LONGUET-HIGGINS, M. S. and R. W. STEWART (1960): Changes in the form of short gravity waves on long waves and tidal currents. J. Fluid Mech., **8**, 565-583.

LONGUET-HIGGINS, M. S. and R. W. STEWART (1961): The changes in amplitude of short gravity waves on steady non-uniform currents. J. Fluid Mech., **10**, 529-549.

LONGUET-HIGGINS, M. S. and R. W. STEWART (1964): Radiation stress in water waves ; A physical discussion, with application. J. Fluid Mech., **11**, 529-562.

OH, I. S., T.-R. KIM, C. Y. CHUNG, and J. H. BONG (1990): A study on the development of shallow water wave model. J. Korea Meteorol. Society, **26**, 139-155.

OGURA, S. (1933): The tides in the seas adjacent to Japan. Hydrogr. Bull. Dept. Imp. Jap. Navy, **7**, 1-189.

PEREGRINE, D. H. (1976): Interaction of water waves and currents. Adv. Appl. Mech., **16**, 9-117.

PHILLIPS, O. M. (1969): The dynamics of the upper ocean, 1st ed., Cambridge University Press, 261 pp.

THOMAS, G. P. (1981): Wave-current interactions; an experimental and numerical study. Part 1. Linear waves. J. Fluid Mech., **110**, 457-474.

TOLMAN, H. L. (1990): The influence of unsteady depths and currents of tides on wind-wave propagation in shelf seas. J. Phys. Oceanogr., **20**, 1166-1174.

YOUNG, I. R. (1988): A shallow water spectral wave model. J. Geophys. Res., **93(C5)**, 5113-5129.

VINCENT, C. E. (1979): The interaction of wind generated sea waves with tidal currents. J. Phys. Oceanogr., **9**, 748-753.

WANG, H. and W.-C. YANG (1981): Wave spectral transformation measurement at Sylt, North Sea. Coastal Engrg, **5**, 1-34.

WHITHAM, G. B. (1962): Mass, momentum and energy flux in water waves. J. Fluid Mech., **12**, 135-147.